Chemistry & Biology
Article

Two Enzymes Catalyze the Maturation of a Lasso Peptide in *Escherichia coli*

Sophie Duquesne,[1] Delphine Destoumieux-Garzón,[1,2] Séverine Zirah,[1] Christophe Goulard,[1] Jean Peduzzi,[1,*] and Sylvie Rebuffat[1]
[1] Chimie et Biochimie des Substances Naturelles, UMR 5154 CNRS, Muséum National d'Histoire Naturelle, CP 54, 57 rue Cuvier, 75005 Paris, France
[2] Present address: Ecosystèmes Lagunaires, CNRS-Ifremer-Université Montpellier II UMR 5119, Place Eugène Bataillon, 34095 Montpellier Cedex 5, France.
*Correspondence: peduzzi@mnhn.fr
DOI 10.1016/j.chembiol.2007.06.004

SUMMARY

Microcin J25 (MccJ25) is a gene-encoded lasso peptide secreted by *Escherichia coli* which exerts a potent antibacterial activity by blocking RNA polymerase. Here we demonstrate that McjB and McjC, encoded by genes in the MccJ25 gene cluster, catalyze the maturation of MccJ25. Requirement for both McjB and McjC was shown by gene inactivation and complementation assays. Furthermore, the conversion of the linear precursor McjA into mature MccJ25 was obtained in vitro in the presence of McjB and McjC, all proteins being produced by recombinant expression in *E. coli*. Analysis of the amino acid sequences revealed that McjB could possess proteolytic activity, whereas McjC would be the ATP/Mg^{2+}-dependent enzyme responsible for the formation of the Gly1-Glu8 amide bond. Finally, we show that putative lasso peptides are widespread among Proteobacteria and Actinobacteria.

INTRODUCTION

Many molecules from bacteria endowed with a broad spectrum of biological activities are biosynthesized through a cyclization process [1]. Lasso peptides [2] are 16–21 residue naturally occurring peptides that result from both cyclization and acquisition of a typical and complex structure [2–7]. A side chain to backbone cyclization leads to an amide bond between the amino group of an N-terminal Gly/Cys residue and the carboxyl group of a Glu/Asp residue at position 8 or 9. The C-terminal tail of the peptide is irreversibly trapped in the ring, thus forming a lasso. Lasso peptides are classified according to the occurrence or not of disulfide bonds [8]. Class I is formed by peptides that contain four cysteine residues at conserved positions [2, 4], whereas class II is formed by peptides devoid of cysteine, in which position 1 is always occupied by a glycine [3, 5–8]. Most lasso peptides have been isolated from Actinobacteria and were shown to be enzyme inhibitors [2–6]. Recently, a *Rhodococcus* strain was shown to produce class II lasso peptides with antimycobacterial properties [7]. However, little is known about the enzymes involved in the biosynthesis of lasso peptides.

Microcin J25 (MccJ25) is a typical class II lasso peptide [9–11]. It is a gene-encoded antibacterial peptide secreted by *Escherichia coli* AY25 [12, 13] which uses the iron-siderophore receptor FhuA to enter bacteria [14] and inhibits RNA polymerase [15]. The ring part of the MccJ25 lasso structure (Figure 1) results from an amide bond between Gly1 and Glu8, and the C-terminal tail is sterically blocked in the ring by the two bulky aromatic side chains from Phe19 and Tyr20 on each side of the ring [9], thus creating a β hairpin region over the ring. Cyclization and folding into the particularly compact lasso structure provide MccJ25 with exceptional resistance to high temperatures, proteases, and chaotropic agents [16]. They also define the functional regions of the molecule implicated in recognition by the receptor FhuA at the outer membrane of bacteria [14] and inhibition of transcription by targeting the RNA polymerase β′ subunit [15]. These two properties are conferred by the Val11-Pro16 β hairpin [14] and the ring tail [17] of the MccJ25 lasso structure, respectively.

A major advantage provided by MccJ25 for studying the enzymes able to generate lasso peptides is that the genetic determinants required for its production are known. The *mcjABCD* gene cluster required for MccJ25 biosynthesis has been sequenced entirely [18] (Figure 1). The gene *mcjA* encodes the linear 58 residue precursor of MccJ25, whereas *mcjD* encodes an ATP-binding cassette (ABC) transporter involved both in the export of MccJ25 and in the self-protection of the producing strain against the deleterious effects of its microcin. The last two genes, *mcjB* and *mcjC*, encode proteins of unknown functions. However, they are necessary for the production of active MccJ25 and have been proposed to encode the enzymes converting McjA into MccJ25 [19]. This process comprises the cleavage of the precursor, the side chain to backbone cyclization of the resulting C-terminal peptide, and the three-dimensional structure acquisition of the microcin (Figure 1).

In this study, we analyzed the effect of *mcjB* and *mcjC* inactivation/complementation on the production of

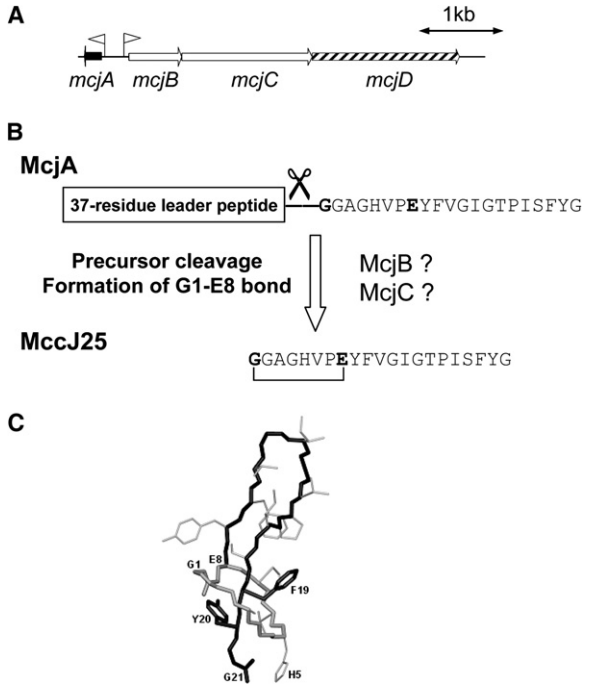

Figure 1. Biosynthesis of MccJ25

(A) Organization of the MccJ25 gene cluster. The genes *mcjA* (black arrow), *mcjB* and *mcjC* (white arrows), and *mcjD* (hatched arrow) encode the MccJ25 precursor McjA, putative maturation enzymes, and the immunity/export protein, respectively. The promoters are indicated by flags.

(B) MccJ25 maturation. McjA is subject to proteolytic cleavage and formation of an amide bond between the amino group of Gly1 and the carboxyl side chain of Glu8.

(C) Three-dimensional structure of MccJ25 (Protein Data Bank code 1Q71).

MccJ25. Furthermore, we cloned and overexpressed McjA, the precursor of MccJ25, as well as McjB and McjC, so as to examine their role in MccJ25 maturation.

RESULTS

McjC Is Expressed as a 513 Residue Protein

The genes *mcjA*, *mcjB*, and *mcjC* were amplified by polymerase chain reaction (PCR) from pTUC202 for cloning into expression vectors. Surprisingly, PCR fragments obtained for *mcjC* systematically displayed a deletion of three bases in the gene encountered in the sequence published for pTUC100, the vector from which the MccJ25 gene cluster was originally sequenced (EMBL accession number AF061787). Following the sequencing of both strands of pTUC202, which derives from pTUC100 [19], it was found that the stop codon located 1327 bases after the initiation codon in the *mcjC* sequence was erroneous (see Figure S1 in the Supplemental Data available with this article online) and was actually displaced 213 bases further (GenBank accession number AM116873). From the sequence data, *mcjC* is separated from *mcjD* by two bases only, and encodes a 513 residue protein (instead of 442) with a molecular mass of 58.7 kDa.

McjB and McjC Are Required for the Production of MccJ25

In order to determine whether *mcjB* and *mcjC* are required for MccJ25 maturation, each gene was inactivated by insertion of a stop codon-containing oligonucleotide duplex at a chosen site in pTUC202 (see Figure S2). The resulting plasmids encoding truncated McjB (127 instead of 208 amino acids) and McjC (52 instead of 513 amino acids) were named pTUC202B and pTUC202C, respectively. Culture supernatants from *E. coli* MC4100 harboring pTUC202, pTUC202B, or pTUC202C plasmids were analyzed for the presence of MccJ25. Whereas the control strain harboring pTUC202 displayed a strong antibacterial activity specifically directed against the MccJ25-susceptible strain, no MccJ25-specific activity could be detected in culture supernatants from strains harboring pTUC202B or pTUC202C (Figure 2). HPLC-MS analysis of the supernatants confirmed that MccJ25, which is characterized by a peak at 10.1 min, was absent from the culture supernatants of strains harboring either pTUC202B or pTUC202C, but present in supernatants from the *E. coli* strain harboring the complete gene cluster (Figure 2). The pellets from strains harboring pTUC202B or pTUC202C were devoid of antibacterial activity (data not shown), which indicated that disruption of either *mcjB* or *mcjC* did not result in export failure but abolished MccJ25 production. The plasmids pET28-*mcjB* and pET28-*mcjC*, encoding His_6-McjB and His_6-McjC, respectively, were further used to complement *E. coli* MC4100 harboring pTUC202B and pTUC202C, respectively. Both antibacterial assays and HPLC-MS experiments clearly demonstrated that MccJ25 production was restored upon complementation (Figure 2). Altogether, these data indicate that both McjB and McjC are required for MccJ25 production. Because the sizes of the inhibition halos produced by complemented strains were smaller than those of wild-type controls, it was speculated that *mcjB* and *mcjC* inactivation had a partial polar effect on their neighbor gene, as one could expect for two genes proposed to be transcriptionally and translationally coupled [18], and as has been observed within the MccC7 gene cluster [20].

Recombinant Expression of His_6-McjA

His_6-McjA was produced as a cytosolic protein in *E. coli* ER2566 harboring pET28-*mcjA*. In the first purification step, using immobilized metal-affinity chromatography (IMAC), His_6-McjA was coeluted with various C-terminally truncated forms due to the high sensitivity of McjA to proteases. An additional RP-HPLC step permitted separation of His_6-McjA from the C-truncated fragments. Purity was checked by MALDI-TOF-MS, which showed two peaks at m/z 8231 and 4117, corresponding to the singly and doubly protonated species, respectively, in agreement with the mass calculated for His_6-McjA (8232 Da; Figure 3A). The yield for His_6-McjA expression and purification was estimated at 150 μg/l of culture. Contrary to MccJ25,

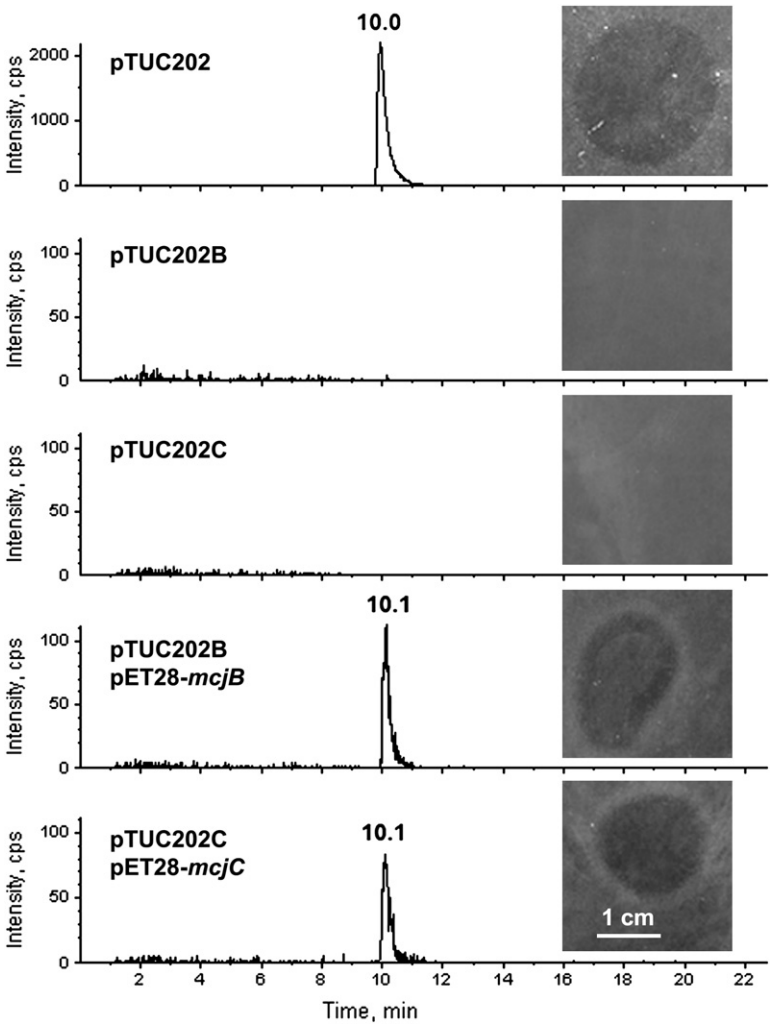

Figure 2. MccJ25 Production Is Abolished upon Inactivation of *mcjB* or *mcjC* and Restored by Complementation

Culture supernatants of *E. coli* MC4100 harboring pTUC202, pTUC202B (inactivated *mcjB*), pTUC202C (inactivated *mcjC*), pTUC202B supplemented with pET28-*mcjB*, and pTUC202C supplemented with pET28-*mcjC* were analyzed by HPLC-MS on a Qq-TOF mass spectrometer. The extracted-ion chromatograms for m/z 703, corresponding to the MccJ25 $[M+3H]^{3+}$ species, are presented together with the antibacterial activities against *S. enterica* serovar Enteritidis. MccJ25 is characterized by the peak at 10.1 min.

His_6-McjA was devoid of antibacterial activity against the MccJ25-susceptible strain (data not shown). The circular dichroism (CD) spectrum of His_6-McjA in aqueous solution displayed a negative band at 198 nm, which indicated the presence of a predominantly random coil conformation (Figure 3B). However, the presence of SDS micelles triggered the folding of the protein, which resulted in two negative bands at 206 and 223 nm, indicative of an α-helical conformation (Figure 3B). Deconvolution of the CD spectrum of His_6-McjA in SDS micelles indicated a helix content in the 10%–15% range.

Recombinant Expression of His_6-McjB and His_6-McjC

His_6-McjB and His_6-McjC were produced in *E. coli* BL21(DE3) harboring pET28-*mcjB* and pET28-*mcjC*, respectively. Generation of inclusion bodies was avoided by growing the strains at 15°C. Soluble His_6-McjB and His_6-McjC purified using IMAC were analyzed by SDS-PAGE. Their electrophoretic mobilities were in accordance with their calculated molecular masses at 26.7 and 60.9 kDa for His_6-McjB and His_6-McjC, respectively (see Figure S3). The identity of the purified proteins was assessed by in-gel digestion with trypsin. The peptide fragments obtained for His_6-McjB and His_6-McjC covered 57% and 30% of the protein sequences, respectively, and were distributed all along the sequences (see Figure S3). The expression/purification yields were estimated at 40 μg and 200 μg/l of culture for His_6-McjB and His_6-McjC, respectively. Given the efficient complementation of inactivated *mcjB* and *mcjC* with DNA sequences encoding His_6-McjB and His_6-McjC (see above), the recombinant proteins were used in further biochemical studies without removal of the N-terminal His tag.

His_6-McjB and His_6-McjC Are Sufficient to Convert His_6-McjA into MccJ25 In Vitro

In vitro reconstitution of MccJ25 biosynthesis was done by incubating His_6-McjA with the potential maturation enzymes His_6-McjB and/or His_6-McjC in the presence of ATP and Mg^{2+}. The ability of both proteins to generate active MccJ25 from its inactive precursor His_6-McjA was monitored by antibacterial assays and HPLC-MS (Figure 4). The incubation of His_6-McjA with either His_6-McjB or His_6-McjC did not generate MccJ25. By contrast, antibacterial activity was detected in the reaction mixture

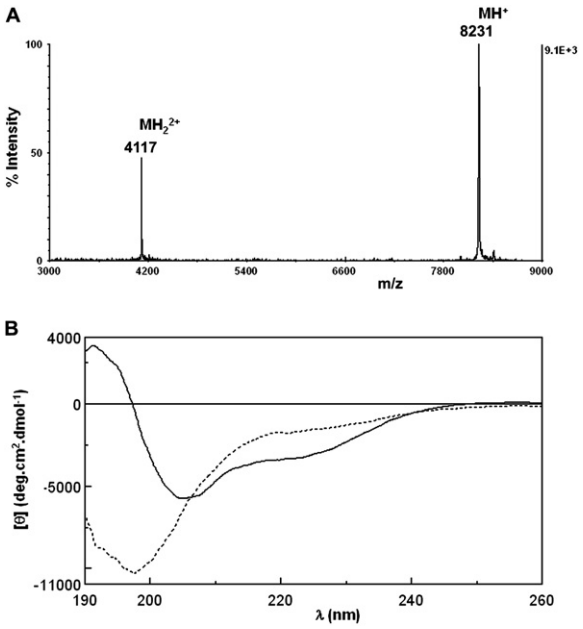

Figure 3. MS and CD Analysis of His_6-McjA

(A) MALDI-TOF spectrum of recombinant His_6-McjA.

(B) CD analysis of His_6-McjA at 75 μM in 10 mM sodium phosphate buffer (pH 7.4) in the absence (dotted line) or presence (solid line) of 8 mM SDS.

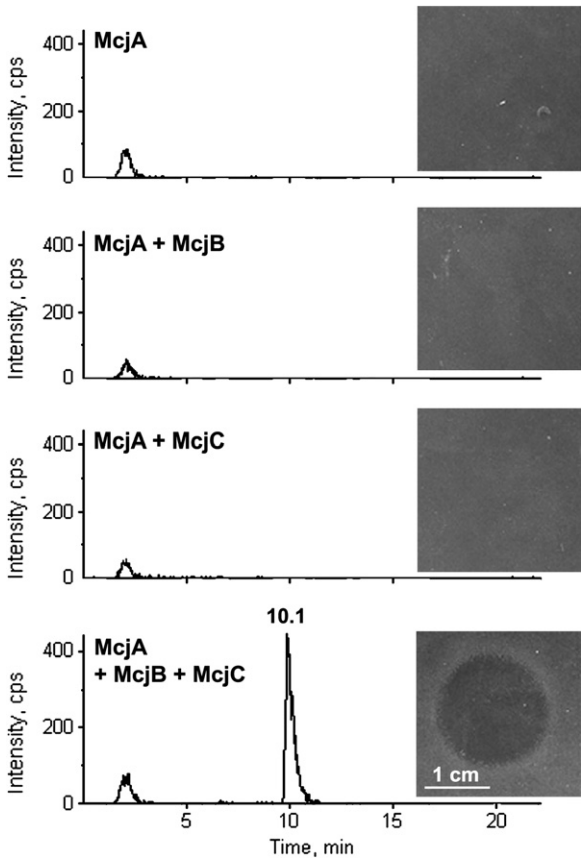

Figure 4. Reconstitution of MccJ25 Biosynthesis In Vitro

HPLC-MS analysis of reaction mixtures containing 0.5 nmol His_6-McjA alone or in the presence of 0.05 nmol His_6-McjB and/or His_6-McjC. The extracted-ion chromatograms for m/z 703, corresponding to the MccJ25 $[M+3H]^{3+}$ species, are presented together with the antibacterial activities against *S. enterica* serovar Enteritidis.

when His_6-McjA was incubated with His_6-McjB and His_6-McjC. This antibacterial activity resulted from the formation of MccJ25, as it was associated with the detection of a triply charged ion at m/z 703 by HPLC-MS, corresponding to the calculated mass for the $[M+3H]^{3+}$ species of MccJ25 (Figure 4). Interestingly, neither antibacterial activity nor MccJ25 could be observed when a synthetic linear MccJ25 corresponding to the 21 residue C-terminal sequence of McjA was used as a substrate instead of His_6-McjA (data not shown).

HPLC-MS/MS analysis of the $[M+3H]^{3+}$ ion of MccJ25 (m/z 703) confirmed that the in vitro-synthesized MccJ25 had acquired a lasso structure, that is, that the C-terminal tail was threaded through the Gly1-Glu8 ring. This could be ascertained given the typical fragmentation pattern of lasso peptides [21]. HPLC-MS/MS profiles of MccJ25 secreted by *E. coli* and the in vitro-synthesized peptide displayed identical retention times and fragmentation patterns (Figure 5). Furthermore, several fragment ions characteristic of the lasso structure were detected at m/z 784.8, 813.4, 869.9, 940.1, and 997.4. Such ions were identified as fragments generated by cleavages within the peptide tail which consisted of tail segments trapped in the Gly1-Glu8 ring, already described for the naturally produced MccJ25 [9, 11].

Factors Affecting the Reconstitution of MccJ25 Biosynthesis

Among different pH and temperature conditions tested for MccJ25 biosynthesis, the best were found to be 25°C and pH 8 (data not shown). Withdrawal of DTT, ATP, or $MgCl_2$ from the reaction mixture impaired the conversion of His_6-McjA into MccJ25 by His_6-McjB and His_6-McjC (data not shown). In order to better characterize the mechanism of MccJ25 synthesis, various protease inhibitors were assayed (for a review of protease inhibitor specificity, see http://www.serva.de/products/sheets/proteases.pdf), and the formation of MccJ25 was monitored by antibacterial assays. Pepstatin A, EDTA, phosphoramidon, leupeptin, and E64 did not prevent MccJ25 biosynthesis. By contrast, AEBSF (4-[2-aminoethyl]-benzenesulfonyl-fluoride), as well as TLCK (1-chloro-3-tosylamido-7-amino-2-heptanone) and TPCK (1-chloro-3-tosylamido-4-phenyl-2-butanone), totally inhibited the formation of MccJ25 (data not shown).

Comparative Analysis of Amino Acid Sequences Involved in the Maturation of MccJ25

In order to predict the function of each protein, similarity searches were performed for McjA, McjB, and McjC amino acid sequences using BLAST programs.

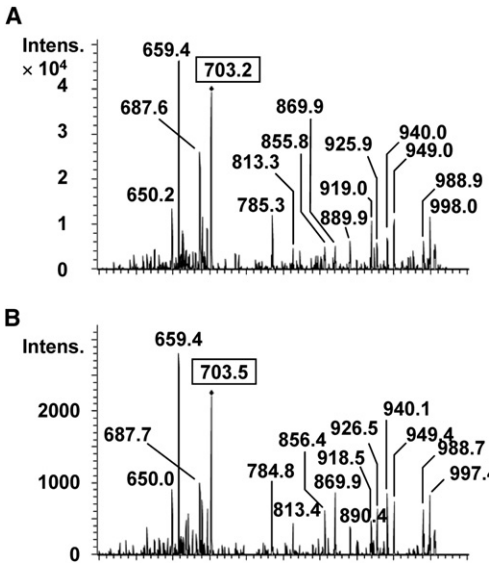

Main Fragment ions	Charge state	Calculated *m/z*	Measured *m/z*
$[G^1\text{-}P^{16}][S^{18}\text{-}G^{21}]\text{-}H_2O$	3	659.32	659.4
$[G^1\text{-}V^{11}][S^{18}\text{-}G^{21}]$	2	784.86	784.8
$[G^1\text{-}G^{12}][S^{18}\text{-}G^{21}]$	2	813.37	813.4
$[G^1\text{-}G^{12}][I^{17}\text{-}G^{21}]$ - CO	2	855.92	855.9
$[G^1\text{-}G^{12}][I^{17}\text{-}G^{21}]$	2	869.92	869.9
$[G^1\text{-}G^{12}][P^{16}\text{-}G^{21}]$	2	918.44	918.5
$[G^1\text{-}T^{15}][S^{18}\text{-}G^{21}]\text{-}H_2O$	2	939.94	940.1
$[G^1\text{-}T^{15}][S^{18}\text{-}G^{21}]$	2	948.95	949.4
$[G^1\text{-}P^{16}][S^{18}\text{-}G^{21}]\text{-}H_2O$	2	988.47	988.7
$[G^1\text{-}P^{16}][S^{18}\text{-}G^{21}]$	2	997.48	997.4
$[G^1\text{-}F^{10}][V^{11}\text{-}G^{21}]$	2	1004.48	1004.1

Figure 5. The In Vitro-Synthesized MccJ25 Is a Lasso Peptide

Collision-induced dissociation spectra of the triply charged m/z 703 precursor ion, obtained from HPLC-MS/MS analysis on an ion-trap instrument of (A) MccJ25 purified from culture supernatants of the *E. coli* MC4100 pTUC202 strain and (B) in vitro-synthesized MccJ25 (product of His_6-McjA incubation with His_6-McjB and His_6-McjC). The main fragment ions consisting of two sterically linked peptides (tail fragments trapped in the Gly1-Glu8 ring) are indicated in the table on the right.

McjC (513 residues) exhibits 20%–22% identity (38% similarity) between amino acids 31 and 376 to the C-terminal domain of asparagine synthetase B (AS-B) from various bacteria, including *Burkholderia* species [22, 23]. This domain of AS-B is involved in the synthesis of asparagine from aspartic acid. However, McjC lacks the N-terminal catalytic domain of AS-B which catalyzes the hydrolysis of glutamine to glutamic acid and ammonia. The amino acid sequence of McjC was aligned with those of AS-B from two *Bacillus* species and one *E. coli*, and with a putative AS-B from *Burkholderia thailandensis*. Given the similarity of the Gly1-Glu8 amide bond defining the lasso ring to the amide bond found in β-lactam rings, three β-lactam synthetases (β-LS) were also included in the alignment. These include carbapenam synthetase (CarA) from *Erwinia carotovora* and β-LS from *Streptomyces clavuligerus* and *Streptomyces cattleya*, which catalyze the formation of a β-lactam ring in carbapenems, clavulanic acid, and thienamycin biosynthetic pathways, respectively [24–26]. Two conserved motifs were identified in the multiple alignment (Figure 6A). These motifs are located in the ATP- and substrate-binding sites of the C-terminal synthetase domain, as deduced from the three-dimensional structures of AS-B, CarA, and β-LS [23, 27–29].

McjB (208 residues) contains two putative functional regions. The N-terminal region up to position 133 is similar (25% identity, 42% similarity) to certain adenosine kinases from mammals. Further, the C-terminal region between amino acids 146 and 200 displays 45% identity (62% similarity) with several hypothetical proteins from Betaproteobacteria (*Burkholderia* species), Alphaproteobacteria (*Caulobacter* species, *Sphingopyxis alaskensis*, *Sphingomonas* sp.), Gammaproteobacteria (*Stenotrophomonas maltophilia*), and Actinobacteria (*Streptomyces avermitilis*), one of which (NCBI RefSeqP ZP_01301928) is referred to as a putative transglutaminase-like enzyme. Among other reactions, transglutaminases catalyze the formation of amide crosslinks between glutamine and lysine residues in proteins [30]. Transglutaminases belong to the large family of cysteine proteases characterized by a Cys-His-Asp catalytic triad [31]. This putative catalytic triad is conserved among McjB and McjB-like proteins from various bacteria (Figure 6B).

Surprisingly, as revealed by BLAST against the peptidase database MEROPS [32], McjA (58 amino acids) exhibits similarities with two regions of a large serine C-terminal processing peptidase-3 from *Flavobacteriales bacterium* HTCC2170 (MEROPS accession number S41.004; NCBI RefSeqP ZP_01105541). However, the active site of this peptidase family is not present in McjA.

Gene clusters similar to that of MccJ25 were found in various bacterial genomes. Neighborhood analysis of McjB-like proteins by the STRING program [33] revealed functional association of an McjB-like protein with both an AS-B (Swiss-Prot accession number Q2SVT9) and an ABC transporter (Swiss-Prot accession number Q2SVT8) in *B. thailandensis* E264. These are similar to McjC and McjD, respectively, and encoded, as in the MccJ25 gene cluster, by two genes located downstream of the *mcjB*-like gene in the complete genome (GenBank accession number CP000086). Moreover, a small open reading frame (ORF) was identified upstream of this *mcjB*-like gene. It encodes a putative 47 amino acid

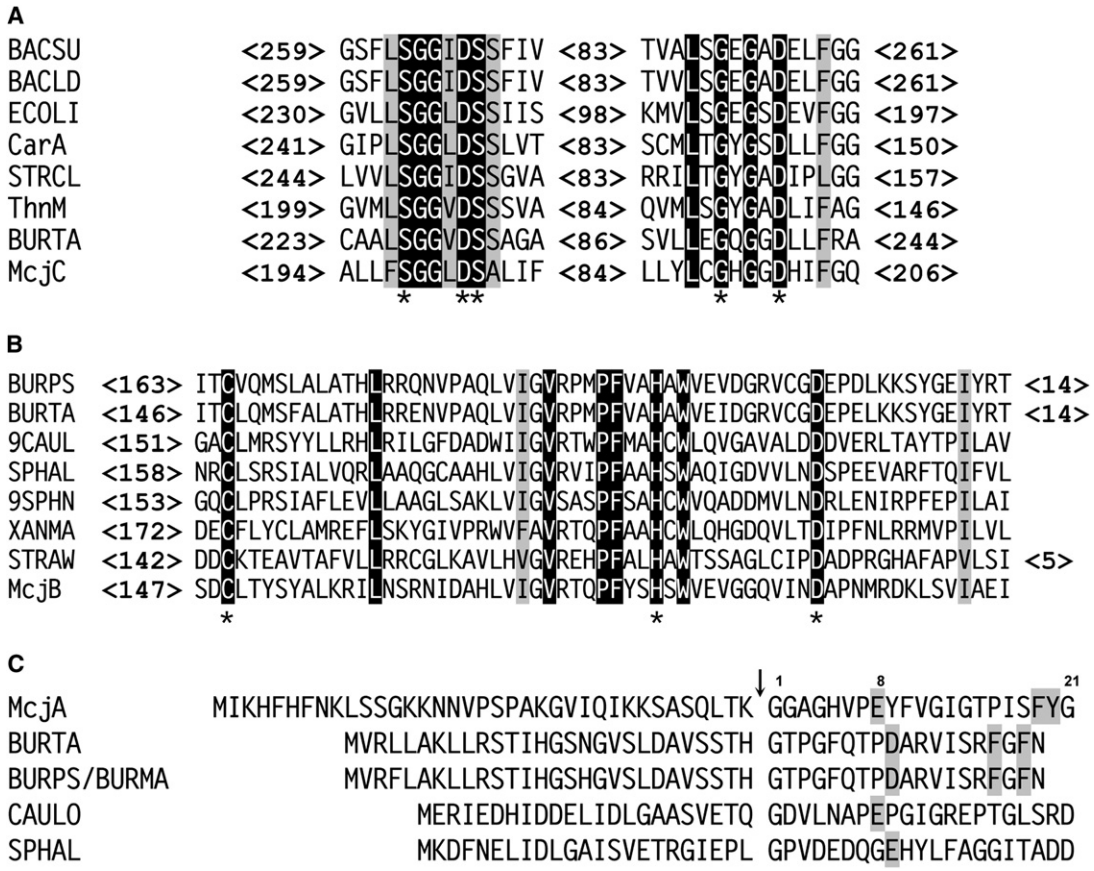

Figure 6. McjC, McjB, and McjA Sequence Similarities

(A and B) Multiple alignments for McjC and McjB. Numbers in angle brackets refer to the length in amino acids of unaligned regions. Letters on black and gray backgrounds highlight identical amino acids and similarity, respectively. All accession numbers of amino acid sequences are from the Swiss-Prot database.

(A) Alignment of similar regions of McjC, asparagine synthetases B (AS-B), and β-lactam synthetases (β-LS). BACSU, AS-B from *Bacillus subtilis* (P54420); BACLD, AS-B from *Bacillus licheniformis* (Q65FV9); ECOLI, AS-B from *E. coli* (P22106); CarA, carbapenem synthetase from *Erwinia carotovora* (Q9XB61); STRCL, β-LS from *Streptomyces clavuligerus* (Q9R8E3); ThnM, β-LS from *Streptomyces cattleya* (Q83XP1); BURTA, putative AS-B from *Burkholderia thailandensis* (Q2SVT9); and McjC, from *E. coli* (Q333M5; this study). The stars indicate amino acids involved in Mg^{2+} coordination and ATP binding.

(B) Alignment of McjB and McjB-like proteins. The stars indicate the catalytic triad of putative cysteine proteases [31]. McjB-like proteins are BURPS, from *Burkholderia pseudomallei* BPSL1795 (Q63U22); BURTA, from *B. thailandensis* E264 (Q2SVU0); 9CAUL, from *Caulobacter* sp. K31 (Q0LZ71); SPHAL, from *Sphingopyxis alaskensis* (Q1GPW3); 9SPHN, from *Sphingomonas* sp. SKA58 (Q1NGU8); XANMA, from *Stenotrophomonas maltophilia* (A1FRG0); STRAW, from *Streptomyces avermitilis* (Q82L14); and McjB, from *E. coli* (Q9X2V8).

(C) Alignment of the MccJ25 precursor, McjA (Q9X2V7), with putative peptides whose C-terminal region displays conserved features of lasso peptides. BURTA, 47 amino acid peptide from *B. thailandensis*; BURPS and BURMA, 47 amino acid peptide from *B. pseudomallei* and *B. mallei*, respectively; CAULO, 44 amino acid peptide from *Caulobacter* sp. K31 (Q0LUL4), SPHAL, 44 amino acid peptide from *Sp. alaskensis*. The arrow indicates the known or putative cleavage site of lasso peptide precursors. Light shading indicates known or putative acid and aromatic residues involved in the amide bond and trapping of the tail in the ring, respectively.

peptide with a 19 residue C-terminal sequence reminiscent of lasso peptide sequences (Figure 6C). In this putative lasso peptide sequence, an N-terminal glycine can be involved in an amide bond with the side chain of aspartic acid at position 9, while, as in MccJ25, two aromatic amino acids (Phe16 and Phe18) located within the C terminus could be involved in the trapping of the tail in the ring. Similar gene clusters encoding the same putative lasso peptide were identified in *Burkholderia pseudomallei* K96243, 1710b, 668, and 1106a and *Burkholderia mallei* ATCC23344 complete genomes (GenBank accession numbers BX571965, CP000124, CP000570, CP000572, and CP000010, respectively). However, an *mcjD*-like gene is lacking in the *B. mallei* genome. It is noteworthy that, contrary to the MccJ25 gene cluster (Figure 1A), the gene clusters encountered in *Burkholderia* species are organized in a single transcription unit. Finally, other putative lasso peptide gene clusters were identified in *Caulobacter* sp. K31 (GenBank accession number AATH01000007) and *Sp. alaskensis* RB2256 (GenBank accession number CP000356) genomes, but, like *B. mallei*, the *mcjD*-like genes are lacking.

DISCUSSION

The unusual lasso three-dimensional structure of MccJ25 has been the subject of major interest [9–11]. In this article, we show that only two enzymes encoded by the MccJ25 gene cluster, namely McjB and McjC, are sufficient for the conversion of McjA, the 58 residue linear precursor of MccJ25, into the lasso-structured MccJ25 endowed with antibacterial activity. To our knowledge, this is the first example of the in vitro reconstitution of a lasso peptide biosynthesis.

A major result from this article is that no other protein but McjB and McjC is necessary to convert McjA into MccJ25. This was clearly shown here by the in vitro generation of a lasso-structured and biologically active MccJ25 from the inactive linear His_6-McjA upon addition of His_6-McjB and His_6-McjC. It therefore appears that the MccJ25-dedicated maturation machinery is encoded by the MccJ25 gene cluster alone. It thus differs from other class I microcins [13], namely microcin B17 (MccB17) and microcin C7/C51 (MccC7/C51), whose precursors are cleaved by proteases that are not encoded by their respective gene cluster but are either chromosome encoded by the producing bacteria (MccB17) or expressed by the target bacteria (MccC7/C51). A relevant inference from our in vitro data is that MccJ25 maturation is completely independent of the export mechanism. Indeed, McjD, which is responsible for the export of MccJ25 into the extracellular medium, is not required to convert His_6-McjA into MccJ25. This finding contrasts with the processing of class II microcins, which requires the complete export machinery to cleave the precursor from its leader peptide concomitant with secretion [13].

The respective function of McjB and McjC was examined using *mcjB*- or *mcjC*-mutated strains. Indeed, in the hypothesis of two enzymes working independently, one of the mutated strains would be expected to accumulate unprocessed McjA while the other would produce linear MccJ25. Unfortunately, we could not detect either McjA or linear MccJ25 in cell pellets and culture supernatants from these strains. However, it cannot be ruled out that inactivation of *mcjB* or *mcjC* affects *mcjA* transcription. The genes *mcjA* and *mcjBCD* are two independent transcription units (Figure 1A), and rapid intracellular degradation of McjA or linear MccJ25 could explain their absence in pellets and supernatants, as observed during the purification of His_6-McjA. Similarly, instability of microcin precursors in strains deficient for the processing machinery has been reported for the precursors of MccB17 and microcin V [34, 35].

Insight into the molecular mechanisms of MccJ25 maturation was obtained by similarity searches and multiple alignments for McjB and McjC. Given its similarity to AS-B and β-LS, McjC is likely to be involved in the formation of the amide bond between Gly1 and Glu8. MccJ25 maturation requires ATP and Mg^{2+}, as AS-B and β-LS do [23, 25, 27–29]. Therefore, we propose that McjC belongs to the family of ATP/Mg^{2+}-dependent amide synthesizing enzymes. Because AS-B and β-LS catalyze intermolecular and intramolecular amide bond formation, respectively, McjC catalytic function is more related to β-LS. As with these enzymes [27–29, 36, 37], the reaction would involve an Mg^{2+}-facilitated adenylation of the γ-carboxylate of Glu8, followed by cyclization via a tetrahedral transition state or an oxyanion intermediate. Based on the conservation of residues located in the β-LS catalytic site (Figure 6A) [23, 27–29], it can be inferred that the side-chain oxygens of Asp203 and Asp302 from McjC coordinate the Mg^{2+} ion, which also interacts with the negatively charged phosphates from ATP. Furthermore, the amide nitrogen of Gly298 and the side-chain hydroxyl groups of Ser199 and Ser204 can interact with adenosine and phosphates from ATP, respectively.

The enzyme responsible for McjA proteolytic cleavage could not be unambiguously identified from this study. On the one hand, we showed that the C-terminal region of McjB contains the Cys150-His182-Asp194 putative catalytic triad of cysteine proteases. On the other hand, MccJ25 in vitro synthesis was blocked by serine protease inhibitors rather than cysteine protease inhibitors. Therefore, the catalytic triad might not involve Cys150 but rather Ser154, located nearby. Further, an autolytic activity of McjA in complex with McjB and McjC cannot be ruled out at this stage, as McjA displays some features of a serine C-terminal processing peptidase-3.

Note that, given the steric trapping of the C-terminal tail in the Gly1-Glu8 ring in MccJ25, the amide bond formation requires the previous positioning of the (1) Gly1 amino group and Glu8 carboxylate and (2) Phe19 and Tyr20 aromatic side chains. As only McjB and McjC are responsible for MccJ25 maturation, the correct positioning of the C-terminal tail is likely to result from the interaction of McjA with one of the modification enzymes, and not to rely on a chaperone protein.

Contrary to McjA, the 21 residue linear MccJ25 was shown not to be a substrate for His_6-McjB and His_6-McjC, suggesting that the 37 residue leader peptide of McjA is required for the maturation. Therefore, the N-terminal leader peptide of the microcin precursor is likely to be involved in the recognition by the modification enzymes rather than the export machinery. This is similar to MccB17 [34] and in contrast with class II microcins [13].

Several peptides displaying the same internal side chain to backbone linkage as MccJ25 were isolated from microbial sources. Although nothing is known about the biosynthesis of these peptides, their occurrence suggests that similar enzymatic machineries could be involved. In this study, putative lasso peptide gene clusters (either complete or partial) were identified in the genome of several Proteobacteria not belonging to the Enterobacteria. Except for MccJ25, all the previously described [7, 8] and the putative lasso peptides are produced by bacteria widely distributed in nature, especially in soil or water. Thus, the MccJ25 gene cluster may have been acquired from these environmental bacteria. The widespread gene clusters encoding putative lasso peptide machineries suggest their conservation during evolution and raise the question of whether lasso peptides observed in various

bacterial strains are involved in bacterial competitions, that is, whether they display antimicrobial properties.

SIGNIFICANCE

Naturally occurring lasso peptides display a complex structure with a side chain to backbone internal linkage forming an N-terminal ring (8 or 9 residues) in which the C-terminal tail is irreversibly threaded. Most of them are enzyme inhibitors produced by *Streptomyces* species. MccJ25 is such a lasso peptide. Gene-encoded and secreted by *Escherichia coli* AY25, it exerts a potent antibacterial activity by blocking bacterial RNA polymerase. Here we demonstrate that two enzymes, namely McjB and McjC, encoded by genes belonging to the MccJ25 gene cluster act in concert to convert the precursor McjA into MccJ25 through a process that requires ATP and Mg^{2+}. To our knowledge, this is the first in vitro reconstitution of a lasso peptide biosynthesis. Our results question the possibility of a common ribosomal biosynthetic pathway leading to lasso peptides in different Proteobacteria and Actinobacteria involving a catalytic mechanism similar to that of β-lactam synthetases.

EXPERIMENTAL PROCEDURES

Bacterial Strains and Plasmids

Strains and plasmids are described in Table S1. Production of recombinant proteins was done in either *E. coli* BL21(DE3) or *E. coli* ER2566 (Novagen). MccJ25 production as well as gene inactivation and complementation assays were performed in *E. coli* MC4100 (laboratory collection). For *mcjB* and *mcjC* complementation, bacteria were transformed with either the *mcjB*-encoding pET28-*mcjB* plasmid or the *mcjC*-encoding pET28-*mcjC* plasmid (this study; see construction below). Antibiotics were purchased from Sigma and used at the following concentrations: ampicillin, 50 μg/ml; chloramphenicol, 34 μg/ml; kanamycin, 50 μg/ml; and tetracycline, 50 μg/ml.

Antibacterial Assays

MccJ25-specific antibacterial activity was detected by radial diffusion assay against the microcin-susceptible *Salmonella enterica* serovar Enteritidis and the microcin-resistant *E. coli* MC4100 pTUC202. A gel overlay was prepared by inoculating 10 ml M63 medium (6.5 g/l agar) with 10^7 colony-forming units per ml of bacteria in exponential phase of growth. Petri dishes containing 20 ml M63 medium (15 g/l agar) were overlaid with the bacterial suspension. After solidification, fractions to be analyzed (10 μl of boiled culture supernatant or enzymatic reaction mixtures) were placed onto the overlay. After a 16 hr incubation at 37°C, plates were analyzed for the presence of inhibition halos. Fractions inhibitory to *S. enterica* serovar Enteritidis but not to *E. coli* MC4100 pTUC202 were considered to contain MccJ25.

Gene Disruption of *mcjB* and *mcjC*

The plasmid pTUC202 was digested at one single site within *mcjB* with BstXI. Stop codons were inserted at this site (371 bases after the *mcjB* initiation codon) by insertion of an oligonucleotide duplex complementary to the BstXI-generated cohesive ends (see Figure S2). The duplex was generated with two complementary 5′-phosphorylated oligonucleotides (5′-GAGCTCGAGTAATAGTAGGGG-3′ and 5′-TTCCCC CTACTATTACTCGAG-3′) designed to introduce an XhoI site and abolish the BstXI site after insertion. Prior to transformation, pTUC202 plasmids lacking the insert were eliminated by digestion with BstXI. The positive clones were selected by restriction map comparison. One positive clone carrying an inactivated *mcjB* gene was selected for MccJ25 expression studies. A similar strategy was used for *mcjC* disruption. Briefly, pTUC202 was digested with SapI (156 bases after the *mcjC* initiation codon) and ligated to a duplex generated with 5′-phosphorylated oligonucleotides (5′-TAATAGTCACTCGAGAGTA-3′ and 5′-CTCGAGTGACTATTATACT-3′) (see Figure S2). One positive clone carrying an inactivated *mcjC* gene was selected.

Construction of Plasmids Encoding His_6-McjA, His_6-McjB, and His_6-McjC

Plasmids encoding McjA, McjB, and McjC with an N-terminal fusion of six histidines were constructed. Basically, *mcjA*, *mcjB*, and *mcjC* were amplified from pTUC202 using the forward primers mcjANdeI (5′-GCCCATATGATTAAGCATTTTC-3′), mcjBNdeI (5′-CATATGATCC GTTACTGCTTAAC-3′), and mcjCNdeI (5′-CCATATGGAAATATTTAA TGTCAAG-3′), respectively, as well as the reverse primers mcjAXhoI (5′-CTCGAGAATATCAGCCATAGAAAG-3′), mcjBXhoI (5′-CTCGAG CTATATCTCTGCAATAAC-3′), and mcjCXhoI (5′-CTCGAGTTAACC TTTATAATCAATG-3′), respectively. The forward and reverse primers introduced NdeI and XhoI restriction sites (underlined), respectively. PCR reactions, performed in an Eppendorf Mastercycler, included 30 cycles: 94°C for 45 s, 45°C for 45 s, and 72°C for 45 s. The amplified fragments were cloned into the pMOSBlue plasmid (GE Healthcare) for sequencing and subcloned into the pET28b expression vector (Novagen) by NdeI/XhoI double digestion.

Expression and Purification of Recombinant His_6-McjA, His_6-McjB, and His_6-McjC

The pET28b derivatives encoding His_6-McjA, His_6-McjB, and His_6-McjC were used to freshly transform *E. coli* ER2566 (for pET28-*mcjA*) or *E. coli* BL21 (for pET28-*mcjB* and pET28-*mcjC*). Cells were grown at 37°C in LB medium supplemented with kanamycin. At the optical density of 0.6 at 600 nm, 1 mM IPTG (QBiogen) was added and cells were further incubated for 1 hr at 37°C (His_6-McjA) or 16 hr at 15°C (His_6-McjB and His_6-McjC). Cells were harvested by centrifugation at 4°C (5000 × g, 20 min) and resuspended in chilled lysis buffer (50 mM sodium phosphate [pH 8], 500 mM NaCl) supplemented with an EDTA-free protease inhibitor cocktail (Roche), 5 μg/ml DNase (Roche), and 10 μg/ml RNase (Sigma). His_6-McjA-producing cells were heated at 100°C for 10 min to prevent enzymatic degradation. Cells were broken in a French press (Thermo Electron) and cell debris were removed by centrifugation (50,000 × g, 30 min). Supernatants were subjected to affinity chromatography on a HisTrap HP column (GE Healthcare) pre-equilibrated with 20 mM (His_6-McjB and His_6-McjC) or 40 mM imidazole (His_6-McjA) in lysis buffer. After loading of the bacterial lysate supernatants, the resin was washed with 80 mM imidazole in lysis buffer and the His-tagged proteins were eluted by increasing the imidazole concentration to 200 mM. Purification at 4°C was monitored by measuring absorbance at 280 nm.

Fractions containing His_6-McjA were desalted by solid-phase extraction on a SepPak C_8 cartridge (Waters Corporation) pre-equilibrated with 0.1% aqueous TFA (trifluoroacetic acid). The cartridge was washed with 0.1% aqueous TFA prior to elution with 20% and 40% acetonitrile (ACN) in 0.1% aqueous TFA. The 40% SepPak fraction was vacuum dried (SpeedVac; Savant) and His_6-McjA was purified by RP-HPLC on a μBondapak C_{18} column (10 μm, 300 × 3.9 mm; Waters Corporation). Separation was performed at a flow rate of 1 ml/min under the following biphasic gradient: 0%–25% ACN in 0.1% aqueous TFA in 2 min and 25%–45% ACN in 0.1% aqueous TFA in 25 min. Purification was monitored by UV detection at 226 nm and fractions were hand collected. Purity was controlled by SDS-PAGE and MALDI-TOF-MS.

Fractions containing His_6-McjB or His_6-McjC were desalted by extensive dialysis against 50 mM sodium phosphate (pH 8), 100 mM NaCl. Purity was assessed by SDS-PAGE.

Protein Quantification

His_6-McjA was quantified on a Uvikon 932 spectrophotometer (Kontron Instruments), assuming a theoretical molar extinction coefficient of 2560 M^{-1} cm^{-1} at 280 nm. His_6-McjB and His_6-McjC were quantified by the Bradford assay with a Coomassie protein assay kit (Pierce).

SDS-PAGE Analysis

Tris-tricine SDS-PAGE (16.5% acrylamide) was performed for His_6-McjA [38], whereas Tris-glycine SDS-PAGE (10%–12% acrylamide) was performed for His_6-McjB and His_6-McjC [39]. Proteins were visualized by silver or Coomassie blue staining. The molecular-weight markers were a polypeptide standard (Bio-Rad) for His_6-McjA and a broad-range protein marker (New England Biolabs) for His_6-McjB and His_6-McjC.

In-Gel Trypsin Digestion

Protein bands were excised from SDS-PAGE and washed twice with 25 mM NH_4HCO_3 (pH 8), once with 50% ACN in 25 mM NH_4HCO_3 (pH 8), once again with 25 mM NH_4HCO_3 (pH 8), and finally with H_2O before being vacuum dried. Gel slices were rehydrated with 50 μl digestion buffer (25 mM NH_4HCO_3 [pH 8.0], 5 mM $CaCl_2$ containing 20 ng/μl trypsin from bovine pancreas [Sigma T8642]) and incubated for 16 hr at 37°C with vigorous shaking. Supernatants were collected. Gels were washed once with 0.1% aqueous FA (formic acid) and once with ACN, and extracts were combined to the formerly collected supernatants. The pooled supernatants were vacuum dried, resuspended in 15 μl 0.1% aqueous FA, and desalted on C_{18} tips (Omix; Varian) before MALDI-TOF-MS analysis.

In Vitro Enzymatic Assays for MccJ25 Synthesis

Freshly prepared His_6-McjA or linear MccJ25, the 21 residue C-terminal sequence of McjA [16] (0.5 nmol), was incubated for 150 min at 25°C in the absence or presence of 0.05 nmol His_6-McjB and/or His_6-McjC in 50 mM sodium phosphate (pH 8), 1 mM DTT, 1 mM ATP, 1 mM $MgCl_2$ (1 ml). To determine the nature of the enzymatic activities, different protease inhibitors were added to the reaction mixture, namely AEBSF (0.25 mM), TPCK (3.5 μM), TLCK (3.5 μM), E64 (12.5 μM), leupeptin (2.5 μM), phosphoramidon (12.5 μM), EDTA (0.5 mM), or pepstatin (25 μM). All were from Sigma, except AEBSF (Alexis Biochemicals). Assays were also done in the absence of ATP or $MgCl_2$, or at 15°C or 25°C, or pH 5 or 7. Solid-phase extraction on SepPak C_8 cartridges (Waters Corporation) was performed for desalting. The reaction mixtures, acidified with 0.1% aqueous FA, were loaded and successively eluted with 5 ml 0.1% aqueous FA, and 5 ml 10% ACN and 3 ml 90% ACN in 0.1% aqueous FA. The last fraction was vacuum dried and resuspended in 50 μl 10% ACN in 0.1% aqueous FA prior to HPLC-MS analysis.

MALDI-TOF Mass Spectrometry

Experiments were done on a Voyager DE-PRO or a 4800 TOF/TOF instrument (Applied Biosystems). One microliter of matrix solution (α-cyano-4-hydroxycinnamic acid or sinapinic acid dissolved at 10 mg/ml in 30% ACN in 1% aqueous FA) was mixed with 1 μl of protein solution or 1 μl of trypsin digest. The mass spectrometer was operated in positive-ion mode with a 25 kV accelerating voltage, either in reflectron mode for His_6-McjB and His_6-McjC trypsin digests or in linear mode for His_6-McjA. The mass spectrometer was calibrated either internally with the ions corresponding to trypsin autodigestion for trypsin digests or externally with a peptide mixture (calibration mixture 3; Applied Biosystems) for His_6-McjA.

HPLC-MS and HPLC-MS/MS Experiments

HPLC-MS experiments were done on a Perkin Elmer chromatographic system (Series 200) connected to an Agilent 1100 UV detector and a Q-STAR Pulsar Qq-TOF mass spectrometer equipped with an ionspray source (Applied Biosystems). The separation was achieved on a Hypersil Gold C_{18} column (1.9 μm, 50 × 2.1 mm; Thermo Electron). The elution gradient was 10%–60% ACN in 0.1% FA over 10 min at a flow rate of 0.25 ml/min. The UV detection was set up at 226 nm and a post-UV split directed 50 μl/min of the effluent to the MS instrument, operated in positive mode over the range m/z 250–1500. HPLC-MS/MS experiments were done on the species at m/z 703 with a 22.5 V collision energy. Alternatively, HPLC-MS and HPLC-MS/MS experiments were conducted on an Agilent 1100 series HPLC system connected to an Esquire 3000 ion trap mass spectrometer equipped with an electrospray ionization (ESI) source, with the same separation conditions. HPLC-MS/MS experiments were done on the species at m/z 703 with a resonant excitation amplitude of 0.85 V_{P-P}.

Circular Dichroism

CD spectra were acquired on a Jasco J-810 spectropolarimeter equipped with a PFD 423S/L Peltier-type temperature controller. His_6-McjA samples, dissolved at 75 μM in 10 mM sodium phosphate buffer (pH 7.4) in the absence or presence of 8 mM SDS, were placed in a 0.05 cm path quartz cell and analyzed at 25°C over the 190–250 nm range. The spectra were acquired at 50 nm/min, with 1 s response time, 2 nm band width, and three scans averaged per sample. CD contribution from the buffer was subtracted, and CD signals were normalized to protein concentration and expressed as the mean residue weight ellipticity, [θ]. The CD spectra were deconvoluted with the different programs provided by DICHROWEB [40], DICHROPROT [41], and CDPro [42] to assess the helix content in the protein structure.

Sequence Analysis

Similarity searches for McjB and McjC (this study) were performed using the BLAST programs [43, 44] at the National Center for Biotechnology Information. Multiple sequence alignment was performed using the CLUSTAL W program [45] with the Gonnet 250 matrix to find highly conserved amino acid sequences. ORFs of more than 100 bases were predicted by ORF Finder at NCBI followed by a similarity search with BLASTP. Searches of proteins associated with McjB-like proteins were performed using the STRING (Search Tool for the Retrieval of Interacting Proteins) program [33] at the European Molecular Biology Laboratory (http://string.embl.de/). Searches for genes neighboring the *mcjB*-like genes were also performed manually. Putative proteolytic activity of McjA was investigated by a BLASTP search against the peptidase database MEROPS [32] at the Sanger Institute (http://merops.sanger.ac.uk/).

Supplemental Data

Supplemental Data include three figures and one table and can be found with this article online at http://www.chembiol.com/cgi/content/full/14/7/793/DC1/.

ACKNOWLEDGMENTS

We are very grateful to Prof. Mohamed A. Marahiel (Philipps-Universitat Marburg, Germany) for constant interest and fruitful discussion on the results reported. We thank Prof. Felipe Moreno (Hospital Ramón y Cajal, Madrid, Spain) for the *E. coli* strain harboring pTUC202 kindly provided. We thank the mass spectrometry facility at the National Museum of Natural History for access to the ESI Qq-TOF instrument, Prof. Jean-Claude Tabet (Université Paris VI, CNRS UMR 7613, Paris, France) for access to the ESI ion-trap mass spectrometer, and Dr. Jean-Michel Camadro (Institut Jacques Monod, France) for access to the MALDI-TOF/TOF instrument. We gratefully acknowledge Dr. Michael Marden (INSERM U473, Le Kremlin Bicêtre, France) for access to the circular dichroism facility. We thank Gérard Gastine for careful technical assistance in bacteriology.

Received: April 12, 2007
Revised: June 1, 2007
Accepted: June 5, 2007
Published: July 27, 2007

REFERENCES

1. Craik, D.J., Daly, N.L., Saska, I., Trabi, M., and Rosengren, K.J. (2003). Structures of naturally occurring circular proteins from bacteria. J. Bacteriol. *185*, 4011–4021.
2. Katahira, R., Yamasaki, M., Matsuda, Y., and Yoshida, M. (1996). MS-271, a novel inhibitor of calmodulin-activated myosin light chain kinase from *Streptomyces* sp.—II. Solution structure of MS-271: characteristic features of the "lasso" structure. Bioorg. Med. Chem. *4*, 121–129.
3. Wyss, D.F., Lahm, H.W., Manneberg, M., and Labhardt, A.M. (1991). Anantin—a peptide antagonist of the atrial natriuretic factor (ANF). II. Determination of the primary sequence by NMR on the basis of proton assignments. J. Antibiot. (Tokyo) *44*, 172–180.
4. Frechet, D., Guitton, J.D., Herman, F., Faucher, D., Helynck, G., Monegier du Sorbier, B., Ridoux, J.P., James-Surcouf, E., and Vuilhorgne, M. (1994). Solution structure of RP 71955, a new 21 amino acid tricyclic peptide active against HIV-1 virus. Biochemistry *33*, 42–50.
5. Katahira, R., Shibata, K., Yamasaki, M., Matsuda, Y., and Yoshida, M. (1995). Solution structure of endothelin B receptor selective antagonist RES-701-1 determined by ^{1}H NMR spectroscopy. Bioorg. Med. Chem. *3*, 1273–1280.
6. Kimura, K., Kanou, F., Takahashi, H., Esumi, Y., Uramoto, M., and Yoshihama, M. (1997). Propeptin, a new inhibitor of prolyl endopeptidase produced by Microbispora. I. Fermentation, isolation and biological properties. J. Antibiot. (Tokyo) *50*, 373–378.
7. Iwatsuki, M., Tomoda, H., Uchida, R., Gouda, H., Hirono, S., and Omura, S. (2006). Lariatins, antimycobacterial peptides produced by *Rhodococcus* sp. K01-B0171, have a lasso structure. J. Am. Chem. Soc. *128*, 7486–7491.
8. Rebuffat, S., Blond, A., Destoumieux-Garzón, D., Goulard, C., and Peduzzi, J. (2004). Microcin J25, from the macrocyclic to the lasso structure: implications for biosynthetic, evolutionary and biotechnological perspectives. Curr. Protein Pept. Sci. *5*, 383–391.
9. Rosengren, K.J., Clark, R.J., Daly, N.L., Goransson, U., Jones, A., and Craik, D.J. (2003). Microcin J25 has a threaded sidechain-to-backbone ring structure and not a head-to-tail cyclized backbone. J. Am. Chem. Soc. *125*, 12464–12474.
10. Bayro, M.J., Mukhopadhyay, J., Swapna, G.V., Huang, J.Y., Ma, L.C., Sineva, E., Dawson, P.E., Montelione, G.T., and Ebright, R.H. (2003). Structure of antibacterial peptide microcin J25: a 21-residue lariat protoknot. J. Am. Chem. Soc. *125*, 12382–12383.
11. Wilson, K.A., Kalkum, M., Ottesen, J., Yuzenkova, J., Chait, B.T., Landick, R., Muir, T., Severinov, K., and Darst, S.A. (2003). Structure of microcin J25, a peptide inhibitor of bacterial RNA polymerase, is a lassoed tail. J. Am. Chem. Soc. *125*, 12475–12483.
12. Salomón, R.A., and Farías, R.N. (1992). Microcin 25, a novel antimicrobial peptide produced by *Escherichia coli*. J. Bacteriol. *174*, 7428–7435.
13. Duquesne, S., Destoumieux-Garzón, D., Peduzzi, J., and Rebuffat, S. (2007). Microcins, gene-encoded antibacterial peptides from Enterobacteria. Nat. Prod. Rep., in press.
14. Destoumieux-Garzón, D., Duquesne, S., Peduzzi, J., Goulard, C., Desmadril, M., Letellier, L., Rebuffat, S., and Boulanger, P. (2005). The iron-siderophore transporter FhuA is the receptor for the antimicrobial peptide microcin J25: role of the microcin Val11-Pro16 β-hairpin region in the recognition mechanism. Biochem. J. *389*, 869–876.
15. Mukhopadhyay, J., Sineva, E., Knight, J., Levy, R.M., and Ebright, R.H. (2004). Antibacterial peptide microcin J25 inhibits transcription by binding within and obstructing the RNA polymerase secondary channel. Mol. Cell *14*, 739–751.
16. Blond, A., Cheminant, M., Destoumieux-Garzón, D., Ségalas-Milazzo, I., Peduzzi, J., Goulard, C., and Rebuffat, S. (2002). Thermolysin-linearized microcin J25 retains the structured core of the native macrocyclic peptide and displays antimicrobial activity. Eur. J. Biochem. *269*, 6212–6222.
17. Semenova, E., Yuzenkova, Y., Peduzzi, J., Rebuffat, S., and Severinov, K. (2005). Structure-activity analysis of microcin J25: distinct parts of the threaded lasso molecule are responsible for interaction with bacterial RNA polymerase. J. Bacteriol. *187*, 3859–3863.
18. Solbiati, J.O., Ciaccio, M., Farías, R.N., Gónzalez-Pastor, J.E., Moreno, F., and Salomón, R.A. (1999). Sequence analysis of the four plasmid genes required to produce the circular peptide antibiotic microcin J25. J. Bacteriol. *181*, 2659–2662.
19. Solbiati, J.O., Ciaccio, M., Farías, R.N., and Salomón, R.A. (1996). Genetic analysis of plasmid determinants for microcin J25 production and immunity. J. Bacteriol. *178*, 3661–3663.
20. Gónzalez-Pastor, J.E., San Millán, J.L., Castilla, M.A., and Moreno, F. (1995). Structure and organization of plasmid genes required to produce the translation inhibitor microcin C7. J. Bacteriol. *177*, 7131–7140.
21. Loo, J.A., He, J.X., and Cody, W.L. (1998). Higher order structure in the gas phase reflects solution structure. J. Am. Chem. Soc. *120*, 4542–4543.
22. Scofield, M.A., Lewis, W.S., and Schuster, S.M. (1990). Nucleotide sequence of *Escherichia coli asnB* and deduced amino acid sequence of asparagine synthetase B. J. Biol. Chem. *265*, 12895–12902.
23. Larsen, T.M., Boehlein, S.K., Schuster, S.M., Richards, N.G., Thoden, J.B., Holden, H.M., and Rayment, I. (1999). Three-dimensional structure of *Escherichia coli* asparagine synthetase B: a short journey from substrate to product. Biochemistry *38*, 16146–16157.
24. McGowan, S.J., Sebaihia, M., Porter, L.E., Stewart, G.S., Williams, P., Bycroft, B.W., and Salmond, G.P. (1996). Analysis of bacterial carbapenem antibiotic production genes reveals a novel β-lactam biosynthesis pathway. Mol. Microbiol. *22*, 415–426.
25. Bachmann, B.O., Li, R., and Townsend, C.A. (1998). β-lactam synthetase: a new biosynthetic enzyme. Proc. Natl. Acad. Sci. USA *95*, 9082–9086.
26. Núñez, L.E., Méndez, C., Braña, A.F., Blanco, G., and Salas, J.A. (2003). The biosynthetic gene cluster for the β-lactam carbapenem thienamycin in *Streptomyces cattleya*. Chem. Biol. *10*, 301–311.
27. Miller, M.T., Bachmann, B.O., Townsend, C.A., and Rosenzweig, A.C. (2001). Structure of β-lactam synthetase reveals how to synthesize antibiotics instead of asparagine. Nat. Struct. Biol. *8*, 684–689.
28. Miller, M.T., Bachmann, B.O., Townsend, C.A., and Rosenzweig, A.C. (2002). The catalytic cycle of β-lactam synthetase observed by X-ray crystallographic snapshots. Proc. Natl. Acad. Sci. USA *99*, 14752–14757.
29. Miller, M.T., Gerratana, B., Stapon, A., Townsend, C.A., and Rosenzweig, A.C. (2003). Crystal structure of carbapenam synthetase (CarA). J. Biol. Chem. *278*, 40996–41002.
30. Lorand, L., and Graham, R.M. (2003). Transglutaminases: crosslinking enzymes with pleiotropic functions. Nat. Rev. Mol. Cell Biol. *4*, 140–156.
31. Makarova, K.S., Aravind, L., and Koonin, E.V. (1999). A superfamily of archaeal, bacterial, and eukaryotic proteins homologous to animal transglutaminases. Protein Sci. *8*, 1714–1719.
32. Rawlings, N.D., Morton, F.R., and Barrett, A.J. (2006). MEROPS: the peptidase database. Nucleic Acids Res. *34*, D270–D272.

33. von Mering, C., Huynen, M., Jaeggi, D., Schmidt, S., Bork, P., and Snel, B. (2003). STRING: a database of predicted functional associations between proteins. Nucleic Acids Res. *31*, 258–261.
34. Madison, L.L., Vivas, E.I., Li, Y.M., Walsh, C.T., and Kolter, R. (1997). The leader peptide is essential for the post-translational modification of the DNA-gyrase inhibitor microcin B17. Mol. Microbiol. *23*, 161–168.
35. Zhang, L.H., Fath, M.J., Mahanty, H.K., Tai, P.C., and Kolter, R. (1995). Genetic analysis of the colicin V secretion pathway. Genetics *141*, 25–32.
36. Bachmann, B.O., and Townsend, C.A. (2000). Kinetic mechanism of the β-lactam synthetase of *Streptomyces clavuligerus*. Biochemistry *39*, 11187–11193.
37. Gerratana, B., Stapon, A., and Townsend, C.A. (2003). Inhibition and alternate substrate studies on the mechanism of carbapenam synthetase from *Erwinia carotovora*. Biochemistry *42*, 7836–7847.
38. Schägger, H., and von Jagow, G. (1987). Tricine-sodium dodecyl sulfate-polyacrylamide gel electrophoresis for the separation of proteins in the range from 1 to 100 kDa. Anal. Biochem. *166*, 368–379.
39. Sambrook, J., Fritsch, E.F., and Maniatis, T. (1989). Molecular Cloning: A Laboratory Manual (Cold Spring Harbor, NY: Cold Spring Harbor Laboratory Press).
40. Whitmore, L., and Wallace, B.A. (2004). DICHROWEB, an online server for protein secondary structure analyses from circular dichroism spectroscopic data. Nucleic Acids Res. *32*, W668–W673.
41. Deleage, G., and Geourjon, C. (1993). An interactive graphic program for calculating the secondary structure content of proteins from circular dichroism spectrum. Comput. Appl. Biosci. *9*, 197–199.
42. Sreerama, N., and Woody, R.W. (2000). Estimation of protein secondary structure from circular dichroism spectra: comparison of CONTIN, SELCON, and CDSSTR methods with an expanded reference set. Anal. Biochem. *287*, 252–260.
43. Altschul, S.F., Madden, T.L., Schaffer, A.A., Zhang, J., Zhang, Z., Miller, W., and Lipman, D.J. (1997). Gapped BLAST and PSI-BLAST: a new generation of protein database search programs. Nucleic Acids Res. *25*, 3389–3402.
44. Schaffer, A.A., Aravind, L., Madden, T.L., Shavirin, S., Spouge, J.L., Wolf, Y.I., Koonin, E.V., and Altschul, S.F. (2001). Improving the accuracy of PSI-BLAST protein database searches with composition-based statistics and other refinements. Nucleic Acids Res. *29*, 2994–3005.
45. Thompson, J.D., Higgins, D.G., and Gibson, T.J. (1994). CLUSTAL W: improving the sensitivity of progressive multiple sequence alignment through sequence weighting, position-specific gap penalties and weight matrix choice. Nucleic Acids Res. *22*, 4673–4680.